Role of deformations and related aspects in super heavy region

Dissertation submitted for partial fulfillment of the requirement for

The award of the degree of

Master of Science

In

PHYSICS

Under

The supervision of

Dr. Manoj Kumar Sharma

(Associate Professor)

Submitted by

Sunil Kumar

Roll no: 300904018

School of physics and Material Science

Thapar University

Patiala – 147004 (Punjab)

Dedicated

To

My Parents

CERTIFICATE

This is to certify that Mr. Sunil Kumar, Roll no 300904018 has worked on this dissertation report as a partial fulfillment for award of the degree of MASTERS OF SCIENCE in physics. I certify that the matter embodied in this report is of candidate's own record and not submitted to any other university in any part or full form for the award of such a degree.

(Dr. Manoj Kumar Sharma)

Supervisor

SPMS, Thapar University

Patiala

Countersigned by:

Dr. O.P. Pandey

(Prof. & Head)

SPMS, Thapar University

Patiala

Dr. S.K.Mohapatra

Dean of Academic Affairs

Thapar University,

Patiala

Acknowledgement

I owe my deepest gratitude to **Dr. Manoj Kumar Sharma**, *my worthy supervisor,* without him the dissertation would not have been possible. I thank him for his patience and encouragement that carried me on through difficult times, and for his insights and suggestions that helped to shape my research skills. I express my sincere thanks to him for his valuable guidance in caring out under his effective supervision, encouragement and cooperation. His visionary thoughts have influenced me greatly. His dynamical attitude has empowered me with zeal of energy to conquer the miner details of my research work.

I also thank **Dr. O.P Pandey, Professor** & Head, school of physics and material science for his support and providing facilities.

A special word of thanks to **Ms. Kirandeep**, research scholar for the help and valuable suggestions whenever I need it out for her busy schedule.

Special thanks to all my friends and the staff at the school of physics and material sciences for providing me a friendly atmosphere and encouraging me throughout this work. I am deeply thankful to my family, their moral support and patient has bared fruit through completion of this thesis.

Sunil Kumar

Roll No: 300904018

Date:

Abstract

In view of present day developments in the domain of nuclear physics, it is extremely important & essential to study the nuclear structure and related aspects at the extreme conditions of angular momentum, deformations, orientations, temperature and energies in reference to the developments in theoretical & experimental nuclear physics. The tough challenges in nuclear perspective can be met only by developing and establishing clear understanding of related phenomena on the theoretical front, which could be utilized to plan and implement the predictions through experiments. A number of factors and properties influence the fusion-fission process and hence need to be handled with proper care in order to make meaningful predictions. One such aspect, which plays a significant role in fusion-fission process dynamics, is the role of deformed shapes of target, projectile and decaying fragments. It is therefore, important to account for shapes of target projectile combinations and the subsequent decaying fragments in the domain of nuclear reaction dynamics.

Keeping this in mind, we have investigated the role of deformations in $^{296}116$ super heavy nuclear system formed in $^{48}Ca+^{248}Cm$ reaction over a wide range of incident energy. The Dynamical Cluster Decay Model (DCM), with deformations up to quadrupole deformations, is used to calculate the fusion evaporation residue cross-section for 3n emission in a hot fusion reaction at various incident energies, taking proton magic number Z=126 and N=184 for super heavy region. The DCM based calculations give good description of measured fusion excitation function, $\sigma_{ER}(=\sigma_{3n})$ as a function of compound nucleus excitation energy E_{CN}, within one parameter fitting, the neck length ΔR (E_{CN}). Some interesting results related to fragmentation behavior and its dependence on nuclear deformations are taken into account for $^{296}116$ nuclear system. The possible implications in reference to temperature and angular momentum effects are addressed in this work.

CHAPTER – 1 INTRODUCTION PAGE NUMBER

CHATER -2 METHODOLOGY

CHAPTER-3

LIST OF FIGURES

LIST OF TABLES

Chapter-1

Introduction

From the early concepts of the atomic and nuclear physics, a nucleus is known as the main core of atoms, consisting of neutrons and protons — which are known as nucleons. These nucleons are binding together by the strong force in spite of the Coulomb repulsion force. They are revolving in the similar way as electrons revolve around the nucleus in the quantized energy states. So many nuclear physicists are trying to understand the force that holds protons and neutrons together, beside this the ordering of nucleons inside the nucleus, and relative stability of nucleons with respect to each other play an important role. The nuclear force is perhaps the only phenomena which have taken almost a century for its understanding and still there are certain issues for which classification are being worked out.

The periodic table of the elements is slowly growing with time. At one time it contained only 92 naturally occurring elements out of which 83 elements are stable and 9 radioactive, starting with Hydrogen (Z=1) and ending with Uranium (Z=92). Majority of these elements have half-lives that are comparable to the age of the Earth, which is about 4.5 billion years old. Since 1940s, however, physicists have been able to produce unstable elements that decay to lighter elements on timescales that can range from thousands of years to tiny fractions of a second. There is, however, more to this branch of physics than simply creating heavier and heavier elements. It is also essential to understand the behavior of these new elements, many of which do not yet have official name.

1.1 Super heavy elements

Super heavy elements — commonly abbreviated as SHE — are known as the transactinide elements, these elements have mass and atomic numbers beyond Uranium, starting from Rutherfordium which has atomic number (Z = 104). Super heavy elements have all been synthesized during the latter half of the 20th century and they are still being produced during the 21st century as high advanced technology [1].

Now the question comes: How these elements beyond Uranium were synthesized: In the synthesis process of heavy elements beyond Uranium the neutrons are added to already existing elements which gets converted into next heavier element by undergoing β-decay process. In step by step process elements are added to the periodic table i.e. a neutron capture followed by β-decay can generate an element of periodic table with higher atomic number. Neutron capture can occur when neutron approaches a nucleus close enough for nuclear forces to be effective so that new isotope is unstable and it decays to emit electrons and neutrino via β-decay process [2].

The way it works is this: we start out with a seed atom placed in a region of high neutron flux, so neutrons start to pile up on seed atom. After collecting some neutrons it become unstable and undergoes beta decay before it can collect any more neutrons. Now neutrons start to collect on the new atom which produces after beta decay with atomic number one greater than the seed atom, and so it goes, stepping through the periodic table [3]. Figure 1.1 shows the formation of compound nucleus via neutron capture and its subsequent decay via gamma and beta particles.

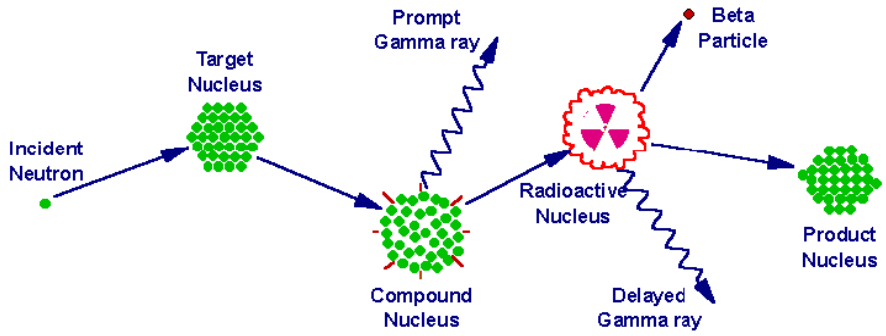

Figure 1.1 Compound nucleus formations via neutron capture and its subsequent decay via γ rays and β particles

1.2 Island of stability and existence of super heavy elements

Island of stability a term from the nuclear physics that described the possibility of elements with particular stable magic no.'s of protons and neutrons. This would allow certain isotopes to be far more stable than other. The idea of island of stability was first proposed by Glenn I Seaborg [4]. The hypothesis is that the atomic nucleus is built up in shell in a manner similar to electrons shells in atoms. In both the cases shells are just group of quantum energy levels that are relatively close to each other. Energy levels from quantum states in two different shells will be separated by

a relatively large energy gap. So, when the number of neutrons and protons completely fill the energy levels of the given shell in the nucleus, the binding energy per nucleon will reach a local maximum and thus that particular configuration will have larger lifetime than nearby isotopes that do have filled shells [5].

According to shell model, these magic numbers are obtained due to spin orbit interaction. Due to the spin orbit interaction the energies of states of the same level are same but with deferent *j* will no longer be identical. This is because in the original quantum numbers, when $\vec{s}$ is parallel to $\vec{l}$, the interaction energy is negative; and in this case *j=l+s =l+1/2*. When $\vec{s}$ is anti-parallel to $\vec{l}$, the interaction energy is positive, and in this case *j=l - s =l -1/2.*[6]

Like due to spin interaction, for n=0, *l* must be 0 and s=1/2 therefore J = 0+1/2 = 1/2 and number of states are determined by the formula: 2J+1 (degenracy), hence 2*1/2 +1=2 states are observed. Similarly for 1p shell n=1, for which *l*=0,1 is observed as *l* varies from 0 to n-1. Therefore two values of total angular momentum are observed j=1/2, 3/2. Due to this splitting of levels take place with 2 protons or neutrons in $1p_{1/2}$ and 4 in $1p_{3/2}$, total 6 states are observed which are shown in figure 1.2

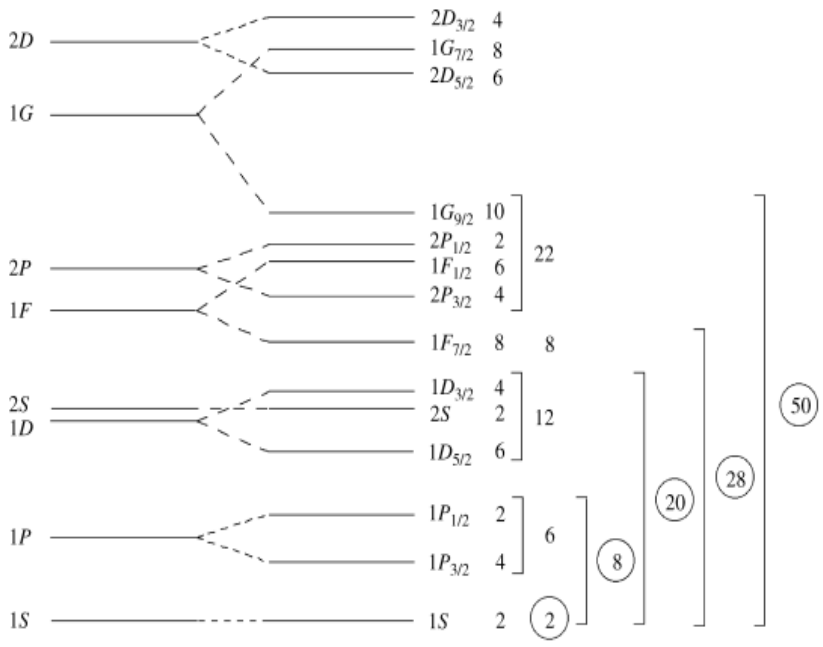

Figure – 1.2 Nuclear energy levels in a potential well obtained with spin-orbit coupling. [7]

Nuclear stability for all nuclei as illustrated in Figure 1.3 is plotted as a function of their number of protons and the number of neutrons. It shows that there are about 300 nuclei which are the most stable nuclei and are located in the valley of stability in the nuclear chart. The existence of the valley of stability is explained by the separation energy of nucleons which is defined as the energy required removing one nucleon (proton or neutron) from the nucleus. The separation energy of a neutron is

$$S_n(N, Z) = B_E(N, Z) - B_E(N - 1, Z).$$

Similarly for the proton, the separation energy is

$$S_p(N, Z) = B_E(N, Z) - B_E(N, Z - 1).$$

By adding neutrons or protons to a nucleus, the nucleus does not accept any more nucleons after a certain number. So at this limit the separation energy of the proton or the neutron has reached zero. These limitations are called proton and neutron drip lines which are placed on the sides of the valley of stability. In the valley of stability, the heaviest stable nucleus is $^{208}_{82}Pb$ with (N = 126, Z = 82) which is a doubly magic nucleus. According to the Nuclear Shell Model, the next doubly magic stable nucleus heavier than Pb is predicted to be at (Z = 114, N = 184) within the sea of instability. This island of stability is so called the region of super heavy elements. That means there exists a number of nuclei around the stable magic nucleus with (Z = 114, N = 184) which are relatively stable nuclei in the sea of instability, the so-called island of stability of super heavy elements and hence 114 is called the stepping stone for super heavy elements in reference to island of stability [8]. Beside Z=114, Z=120 and Z=126 are other completing proton magic numbers in the super heavy region. Now as we have synthesized super heavy nuclei up to Z=117 or 118. So we are hopeful to find some stable nuclear systems in the range of Z=114 –126 & N=178-184, which could be used for numerous applications for the better future.

The most interesting goal of super heavy elements is to answer the question of whether there is a limit for the number of nuclei. The main challenge in nuclear physics is to find the maximum number of protons for which a relatively stable nucleus can exist. This has created a competition between the biggest laboratories in the world. After these challenges and predictions, several

experiments were made to produce and identify super heavy elements in the island of stability [8].

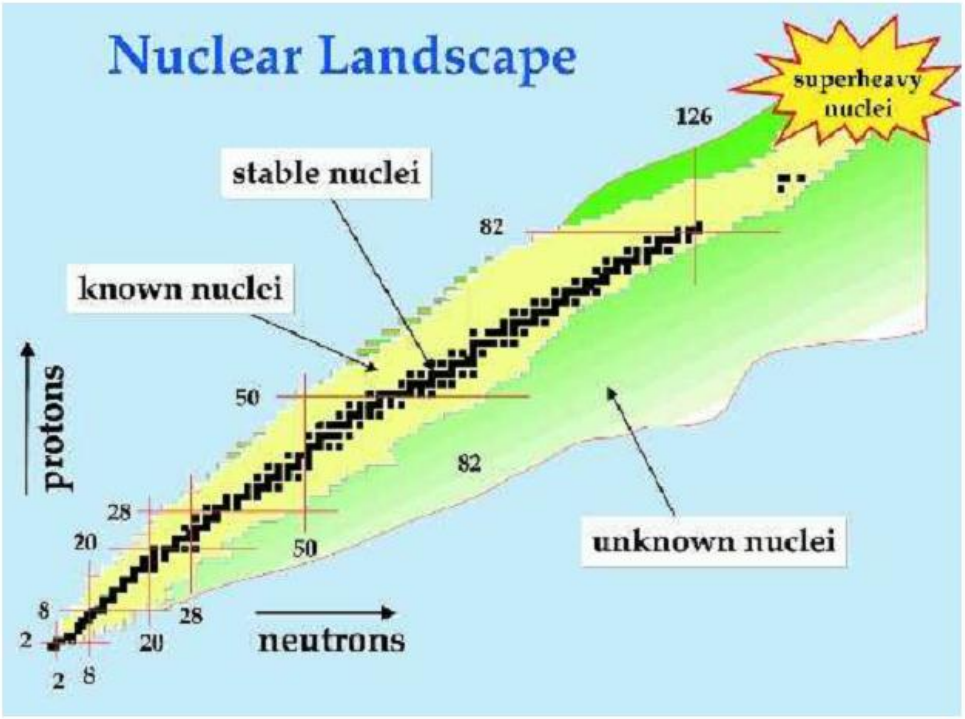

Figure 1.3 nuclear charts [9]

1.3 Nuclear shells and stabilization of super heavy elements

The Nuclear Shell Model has been studied and possesses some predictions in the region of lesser known super heavy elements. It predicts that the next doubly magic nucleus has atomic number Z = 114 or 120 or 126 and neutrons number N=178 or 184. This gives an indication of the existence of stable heavier elements in the island of stability.

According to the Liquid Drop Model, the spontaneous fission barrier is nearly zero for heavy nuclei. But after the correction of the Shell Model of nuclear potential, the fission barrier of this elements is of relatively high of about 6 – 8 MeV. Sequentially, the half-life of these nuclei increases with respect to spontaneous fissions. The number of neutrons increases as we move away from high stability. Nuclear deformation is expected to increase as N increases. A super heavy nucleus is supposed to be formed if its half life time is greater than that of spontaneous fission life time, as expected for Z=114 or 120 or 126 and N=178 or 184 cases. This gives an

indication, if super heavy nuclei have a high stability with respect to spontaneous fission, they will decay to their ground state through different other decays such as neutron decay, alpha decay and possibly beta decay. If there exists or there is possible production of super heavy elements in the trend line of stability, it can be a possible production of a number of super heavy nuclei near the stable magic or double magic nucleus [8].

1.4 Deformed nuclei

Not all nuclei have the spherical shape with closed shells. In the heavy and super heavy mass region, nuclei have non spherical charge distributions even in their ground states. These deformed shapes govern the electric quadrupole moment. These nuclei are away or far away from closed shell with deformation shape; these deformations include additional modes of nuclei to be in excited state with a possible change in of their electric quadrupole moment [10]**.**

1.5 Electric quadrupole moment [11]

Considering the distribution of the nuclear charge ρ(r), the multipole moment is important for determining the nuclear potential at any point p from a distance R away from the nuclear distribution of the nuclear charges as can be shown in figure 1.4

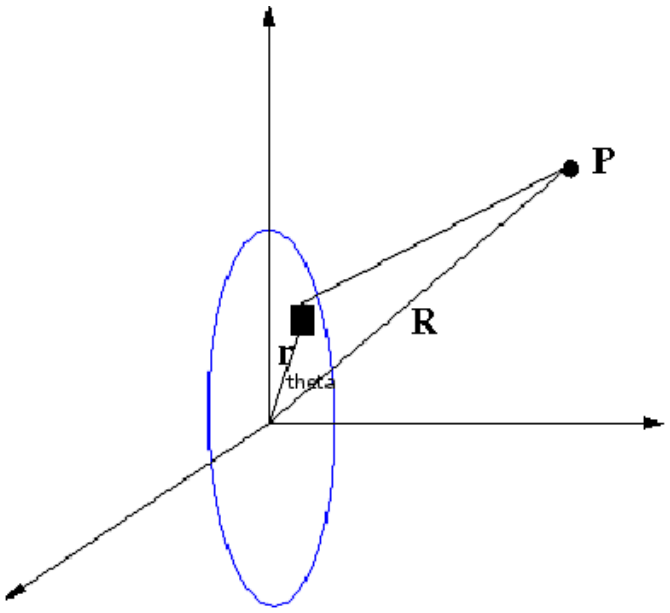

Figure 1.4 Potential of a quadrupole charge distribution

The formula of the potential at position $\vec{r}$

$$V(\vec{r}) = \frac{1}{4\pi\epsilon}\int_{vol}\frac{\rho(\vec{r})}{|\vec{R}-\vec{r}|}d\vec{r}. \qquad \text{----------(A)}$$

Using Taylor series expansion of the potential for small values of $|\overrightarrow{r/\vec{R}}|$ around the origin of the axis of the charge distribution, above equation becomes

$$V(\vec{r}) = \frac{1}{4\pi\epsilon}\frac{q}{R} + \frac{1}{4\pi\epsilon}\int\frac{\rho(\vec{r})r\cos\theta}{R^2}d\vec{r} + \frac{1}{2}.\frac{1}{4\pi\epsilon}\int\frac{\rho(\vec{r})(3\cos^2\theta-1)r^2}{R^3}d\vec{r} + \cdots \qquad \text{----- (B)}$$

From Figure we can determine cosθ as

$$r\cos\theta = \frac{\vec{r}.\vec{R}}{R} = \sum_i x_i X_i/R,$$

Where x_i for i = 1, 2, 3 represent to the Cartesian coordinates. From equation (B), q is the total charge which is defined by $\int_{vol}\rho(\vec{r})d\vec{r}$. Expanding equation (B) in Cartesian coordinates, we obtain

$$V(\vec{r}) = \frac{1}{4\pi\epsilon}\frac{q}{R} + \sum_i\frac{\rho_i X_i}{4\pi\epsilon_0 R^3} + \sum_{ij}\frac{1}{2}\frac{1}{4\pi\epsilon_0 R^3}\frac{Q_{ij}}{R^5 X_i X_j} + \cdots$$

Where

$$\rho_i = \int\rho(\vec{r})x_i d\vec{r},$$

And

$$Q_{ij} = \int\rho(\vec{r})(3x_i x_j - r^2\delta_{ij})d\vec{r}.$$

Where Q_{ij} is so called the quadrupole moment .If $Q_{ij} = 0$, the nuclear charges are distributed uniformly as sphere shape. If quadrupole moment is not equals to zero it give rise to two kinds of shape distributions.

1) It can cause a prolate deformation, making the spherical nucleus actually appear more like a football, positive quadrupole deformations.

2) It can cause an oblate deformation, making the spherical nucleus actually appear more like a doorknob, negative quadrupole deformations.

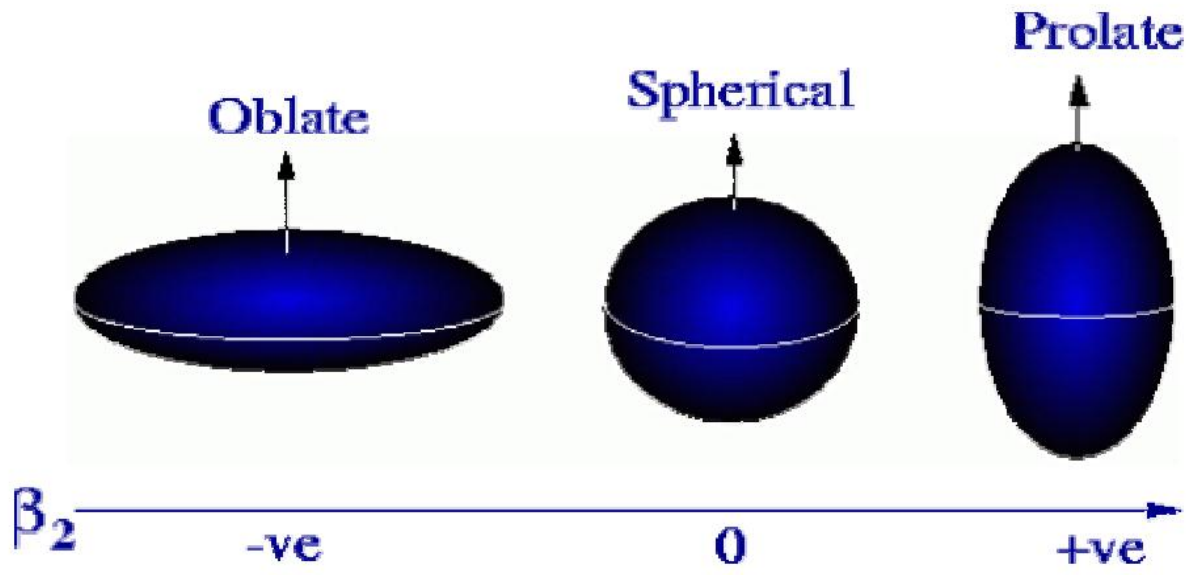

Figure 1.5 Nuclear Shapes for oblate, spherical and prolate nucleus

1.6 Importance of deformed nuclei

The depth and the width of the capture well in the nucleus-nucleus interaction potential, as well as the barrier height are known to play a dominant role in the dynamics of a compound nucleus formed in heavy ion reactions. This feature is associated with the necessity to overcome the barrier that exists between two separated nuclei and with a formation of a scission neck between contacting nuclei in the capture well, as well as with the following evolution of shape of the nuclear system. Therefore, it is very important to study the influence of deformation and orientation on the nucleus-nucleus interaction potential.

It has been observed that when we opt for a deformed target/ projectile combination for the synthesis of heavy/ super heavy nuclei the fusion probability in general gets increased as the barrier gets modified with inclusion of deformation & orientation effects**.**

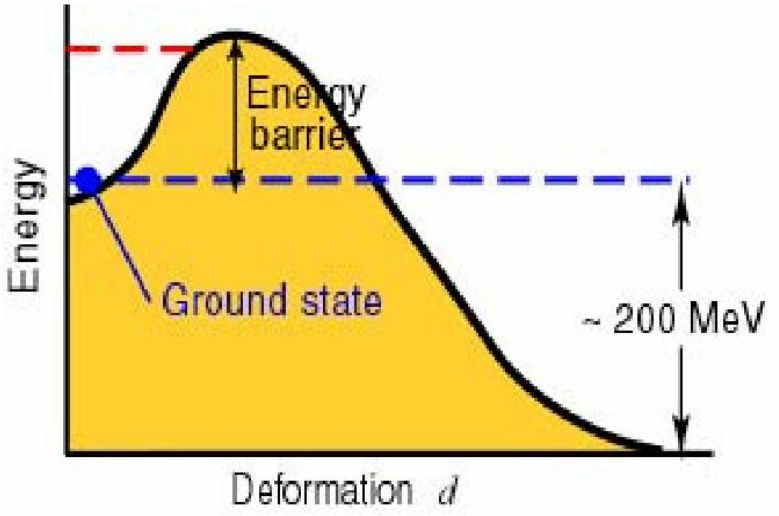

Figure 1.6 Potential Barrier vs. deformation

The apparent reason for this enhancement in fusion probability is that the inclusion of deformation and orientation effects of the colliding nuclei leads to lowering of its barrier height to provide easier path for compound nucleus formation. The collisions between deformed as well as oriented nuclei have been studied theoretically and experimentally to establish the effect of deformation and orientation on fusion reactions [12]-[15], and to explain the deformation effect nicely we have to understand the concepts as explained by Nilsson Model.

1.7 The deformed shell model: Nilsson Model

The Nuclear Shell Model describes only the spherical nuclei. Also, the Shell Model is not able to give a general description of nuclei far away from the spherical closed shell. The Nilsson Model corrects the limitations of the spherical Shell Model and enables a general overview of the single particle states of deformed nuclei. However, the Nilsson Model has dealt only with the quadrupole deformation (either oblate or prolate) by modifying the harmonic oscillator potential with spin orbit coupling; also for single particle, it can be described by using Wood-Saxon potential.

In order to describe the single particle deformed model (Nilsson Model), the total angular momentum and the orbital angular momentum are no longer good quantum numbers. Only the projection of the total angular momentum onto the symmetry axis and the parity are good quantum numbers to describe the energy eigenvalues of the single particle of deformed nuclei. These eigenvalues can only be determined by the principle quantum number, the projection of the total and orbital angular momentum onto the symmetry axis and the parity. The Nilsson Model relies on a deformed harmonic potential, taking into account the angular momentum and the correction of spin-orbit coupling by adding these terms to the potential. The Hamiltonian for a single particle in a deformed nucleus is

$$H = \frac{p^2}{2m} + \frac{1}{2}m\left[\omega_x^2(x^2+y^2) + \omega_z^2\right] - C\vec{l}.\vec{s} - DL^2,$$

Where *P* and *m* are the momentum and the mass of the nucleon respectively, x, y, z are the Cartesian coordinates, *l* and *s* are the orbital and spin angular momentum respectively, and C and D are parameters.

The first term of the equation describes the kinetic energy of the particle, the second term is the anisotropic harmonic oscillator's potential for deformed nuclei, the third term is the spin orbit coupling which lowers the energy levels; the fourth term lowers the energy. The parameters C, D are obtained experimentally. This give a good fit to the experimental data of early days.

In the Nilsson Model, the energy levels depend on the deformation. Energy levels with the same total angular momentum have different energies. So the Nilsson wave function is described by the quantum numbers as $\Omega^{\pi}[Nn_Z\Lambda]$, where z is the symmetry axis, is the projection of the total angular momentum onto the symmetry axis which gives the splitting of the total angular momentum into different energy levels, π is the parity, N is the principle quantum number, n_z is the number of nodes and Λ is the projection of the angular momentum *l* onto z axis (symmetry axis) [11]. With time a lot of development is made on these basic models and deformations have been made available for octupole, hexadecapole and triaxial symmetry shapes. Gupta & collaboration [12]-[15] have done extensive work to understand the effect of nuclear deformation in the formation & decay process of nuclear systems. A versatile model known as Dynamical Cluster Model (DCM) has been worked out and the effects of deformations, orientations, angular

momentum and temperature dependence etc. has been exclusively incorporated in the framework of DCM. We propose to use this model for the dynamics in super heavy region specifically for Z=126 nucleus. The details of DCM are given in chapter 2.

1.8 Synthesis of super heavy elements

Super heavy elements are produced by the bombardment of lighter elements using particle accelerators namely using fusion reaction to create them. For example

$$_{20}Ca^{48} + _{96}Cm^{248} \rightarrow {}_{116}Uuh^{296}$$

Where this symbol Uuh is for the element Ununhexium which has Z = 116. The one of the method of creating super heavy nuclei by using heavier projectiles to bombard target atoms is the cold fusion reaction, by choosing masses and bombardment energies very carefully in order to minimize the excitation of the product nuclei.

Synthesizing heavy elements by fusion reactions requires choosing good methods of projectile and target that yield nuclei with less deformation, and a particularly stable nucleus .The most difficult issue in the experiments is how to choose a reaction that does not yield to an excited nucleus which might decay by fission instead of creating a heavier and stable nucleus. For this reason, Scientists are switching from using light projectiles with heavy targets to less massive targets with relatively heavier projectiles; e.g. using lead-208 or Bismuth-209 with Chromium-54 or iron-58 [8].

1.9 Fusion reactions

Nuclear fusion is the process in which multi atomic nuclei join together to form a heavier nucleus. It is followed by the release or absorption of energy. From Figure 1.7, we can see that iron and nickel nuclei are the most stable nuclei and they have the largest binding energy per nucleon. Therefore, a fusion reaction of nuclei lighter than iron and nickel release energy and reactions of nuclei heavier than iron and nickel absorbs energy. Nuclear fusion occurs naturally in stars and also has been made artificially but it is not completely controlled [16].

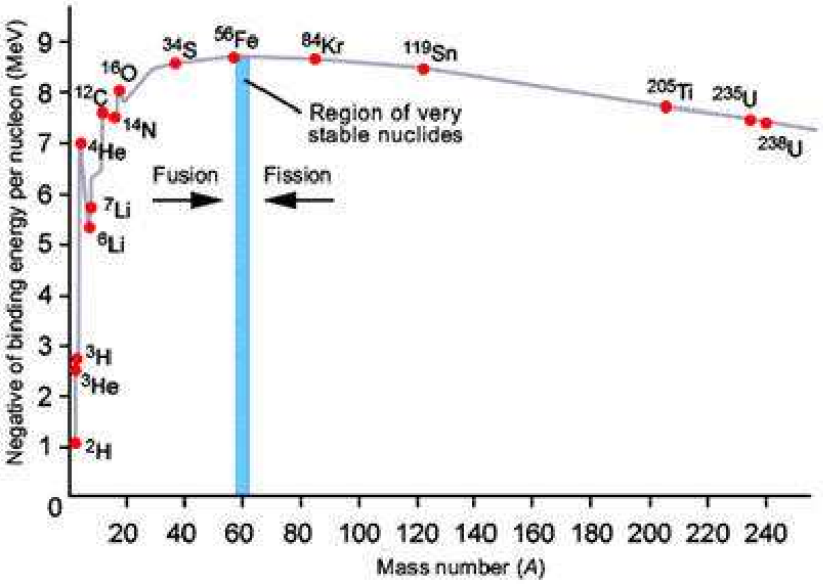

Figure: 1.7 Variation of binding energy with mass number

It is well known that heavy and super heavy nuclei are synthesized in heavy ion fusion reactions. In order to find the mechanism of producing compound nuclei from this reaction, there are two different methods which are cold fusion and hot fusion reactions. These methods only depend on one parameter which is the excitation energy of the compound nucleus that gives a maximum result of the reaction [17].

1.9(a) Cold fusion

In cold fusion reactions, the excitation energy of the fused nuclei remains low after the reactions; it cools down the nucleus to its ground state by emission of only one neutron or gamma rays. This is the main advantage of this type of reactions. Also, the cold fusion method to synthesize super heavy nuclei has a disadvantage because of the Coulomb electrostatic repulsion forces between the two fused nuclei in the fusion reaction. When two nuclei approach each other to interact together, part of their kinetic energy is converted to excitation energy of the collision system led to reduce the energy needed to overcome the fusion barrier and prevents the fusion from occurring.

For example, in the reactions of the fusion of lead-208 (or bismuth-208) magic nuclei with heavy projectiles (mass number 50 − 70), the maximum result of the reaction products with atomic

number (A = 104 − 112) is observed experimentally at a compound nucleus with energy (E = 10 − 20 MeV), respectively.

The first elements with atomic numbers (Z = 107 − 112) were synthesized in cold fusion reactions by studying their properties of radioactive decay chains [8].

Elements formed by cold fusion are [18]:

(1)107 Bohrium: Was the first new element synthesized using methods of in-flight recoil separation. The reaction

$$_{24}Cr^{54} + _{83}Bi^{209} \rightarrow _{107}Bh^{262}$$

(2)108 Hassium: Was synthesized in α- decay chains were measured in the irradiation of Pb^{207}, Hs^{269} was discovered as a link in the decay chain of $112^{277,}$ also in this reaction:

$$_{82}Pb^{208} + _{26}Fe^{58} \rightarrow _{108}Hs^{265} + _{0}n^{1}$$

(3)109 Meitnenium: Was observed in irradiation of Bi^{209} with Fe^{58} by a single α decay chain

$$_{83}Bi^{209} + _{26}Fe^{58} \rightarrow _{109}Mt^{266} + _{o}n^{1}$$

(4)110 Dremstedium: Was discovered using reaction

$$_{28}Ni^{62} + Pb^{208} \rightarrow _{110}Ds^{269} + _{0}n^{1}$$

(5) 111 Roentgenium: Investigated using reaction

$$_{83}Bi^{209} + _{28}Ni^{64} \rightarrow _{111}Rg^{272} + _{0}n^{1}$$

(6)112 Ununbium: It was discovered at GSI

$$_{82}Pb^{208} + _{30}Zn^{70} \rightarrow _{112}Uub^{278} \rightarrow _{112}Uub^{277} + _{0}n^{1}$$

1.9(b) Hot fusion

Using hot fusion reaction to produce super heavy elements always involves a heavy target in the region of actinide nuclei (Pu, Cm) with light projectile nuclei (Ca, Zn). The heavy target includes many protons which give rise to the coulomb barrier. This implies that the projectile must have a high energy to overcome the Coulomb barrier. In order to make very heavy nuclei by a fusion reaction, we need to cool down the hot compound nucleus which has more excitation energy and mostly by evaporation of more neutrons and the emission of gamma ray than cold fusion reaction. The lifetime of these nuclei is limited by the possibility of the fission into two parts.

Using hot fusion reaction, scientist succeeded in producing five super heavy elements which are Nobelium (No; Z = 102), Lawrencium (Lr; Z = 103), Rutherfordium (Rf, Z = 104), Dubnium (Db; Z = 105) and seaborgium (Sg; Z = 106). [19]

Elements Produced by Hot fusion reaction [18]:

(1) 104 Rutherfordium $_{94}Pu^{242} + {}_{10}Ne^{22} \rightarrow {}_{104}Rf^{264}$

(2) 105 Dubnium $^{249}Cf_{98} + {}^{15}N_{7} \rightarrow {}^{260}Db_{105} + 4_{0}n^{1}$

(3) 106 Seaborgium $_{96}Cm^{248} + {}_{10}Ne^{22} \rightarrow {}_{106}Sg^{266} + 4_{0}n^{1}$

(4) 114 Ununquadium $_{20}Ca^{48} + {}_{94}Pu^{244} \rightarrow {}^{114}Uuq^{*292} \rightarrow {}_{114}Uuq^{289} + 3_{0}\, n^{1}$

(5) 115 Ununpentium $_{20}Ca^{48} + {}_{95}Am^{243} \rightarrow {}_{115}Uup^{*291} \rightarrow {}_{115}Uup^{288}$

(6) 116 Ununhexium $_{20}Ca^{48} + {}_{96}Cm^{249} \rightarrow {}_{116}Uuh^{293} + 3_{0}n^{1}$

(7)117 Ununseptium $_{20}Ca^{48} + {}_{97}Bk^{249} \rightarrow 117^{*297} \rightarrow 117^{294} + 3n$

(8) 118 Uunoctium $^{20}Ca^{48} + {}_{98}Cf^{249} \rightarrow {}_{118}Uuo^{294} + 3\,{}_{0}n^{1}$

1.10 General discussion about the super heavy nuclei 116

According to the International Union of Pure and Applied Chemistry (IUPAC), the super heavy element 116, historically known as eka-polonium is called Ununhexium as a temporary name. It

has been added to the periodic table with the temporary symbol Uuh, atomic number 116 and mass number 293 (N = 177). It is located in the periodic table in group fourteen of the chemical elements group with seventh period [20].

Element Uuh-116 has more than an isotope which has the same number of protons and different number of neutrons; all the isotopes were synthesized in different laboratories which are man-made, and some of them were observed as a decay product of element Uunoctium (Z=118) [20].

1.10(a) Production of the super heavy nucleus 116

At the laboratory of Joint Institute for Nuclear Research (JINR) in Dubna, there was a collaboration to produce element 116 by using the reactions

$$_{20}Ca^{48} + {}_{96}Cm^{248} \rightarrow {}^{296}_{116}Uuh^{*} \rightarrow {}^{293}_{116}Uuh + 3^{1}_{0}n$$

$$_{20}Ca^{48} + {}_{96}Cm^{245} \rightarrow {}^{293}_{116}Uuh^{*} \rightarrow {}^{291}_{116}Uuh + 2^{1}_{0}n$$

On July 19, 2000, scientists at Dubna (JINR) detected a single decay from an atom of ununhexium following the irradiation of a Cm-248 target with Ca-48 ions. The results were published in December, 2000 [21]. This 10.54 MeV alpha-emitting activity was originally assigned to ^{292}Uuh due to the correlation of the daughter to previously assigned ^{288}Uuq. However, that assignment was later altered to ^{289}Uuq, and hence this activity was correspondingly changed to ^{293}Uuh.

The table 1.1 shows the different isotopes of Uuh and the corresponding years of discovery

Isotopes	Year discovered	Discovery reaction
^{290}Uuh	2002	^{249}Cf(^{48}Ca,3n)
^{291}Uuh	2003	^{245}Cm(^{48}Ca,2n)
^{292}Uuh	2004	^{248}Cm(^{48}Ca,4n)
^{293}Uuh	2000	^{248}Cm(^{48}Ca,3n)

Table 1.1 different isotopes and years of discovery

Ununhexium has also been observed in the decay of ununoctium. In October 2006 it was announced that 3 atoms of ununoctium had been detected by the bombardment of californium-249 with calcium-48 ions, which then rapidly decayed into ununhexium. [20]

1.10(b) Fission of compound nuclei with Z=116

Several experiments have been performed during 2000 to 2006 at the Flerov laboratory of Nuclear Reactions in Dubna studying the fission characteristics of the compound nuclei ^{296,294,290}Uuh. Four nuclear reactions have been used, namely ^{248}Cm+^{48}Ca, ^{246}Ca+^{48}Ca, ^{244}Pu+^{50}Ti and ^{232}Th+^{58}Fe. The results have revealed how nuclei which goes fission predominantly by expelling closed shell nuclei such as ^{132}Sn (Z=50, N=82). It was also found that the yield for the fusion-fission pathway was similar between ^{48}Ca and ^{58}Fe projectiles, indicating a possible future use of ^{58}Fe projectiles in super heavy element formation [22].

1.10(c) Decay properties of elements 116

After producing heavy nuclei by a certain reaction, these nuclei undergo alpha decay which gives a daughter nucleus with two protons and two neutrons lighter than the parent nucleus. If the daughter nucleus has a low probability against spontaneous fission, it will undergo alpha decay. After a chain of emitting alpha particles, the decay chain will terminate by spontaneous fission into two lighter nuclei [23]. In the region of heavier nuclei, spontaneous fission is predominant according to the macroscopic liquid drop model; the competition between alpha decay and spontaneous fission is the dominant decay modes in this region.

• Alpha decay

Alpha decay is a type of radioactive decay in which an atomic nucleus emits an alpha particle, and thereby transforms (or 'decays') into an atom with a mass number 4 less and atomic number 2 less. The reason alpha decay occurs is because the nucleus has too many protons which cause excessive repulsion in super heavy regions the quantity of protons is very high hence they are extreme good for alpha decay.

The predictions of the half -lives of heavier nuclei are based on the theoretical calculations of the released energy from emitting an alpha particle from a parent nucleus [24]. This released energy

is called Q-value which can be determined from the binding energy of the alpha and the parent nucleus as

$$Q_\alpha = B_E\,(A-4,\, Z-2) + B_E\,(4,\, 2) - B_E\,(A,\, Z)$$

• Spontaneous fission

Spontaneous fission is a form of radioactive decay characteristic of very heavy isotopes. It is theoretically possible for any atomic nucleus whose mass is greater than or equal to 100 atomic mass units (u). In practice, however, spontaneous fission is only energetically feasible for atomic masses above 230 u. According to the LDM spontaneous fission is a predominant decay mode in the region of heavier nuclei, but the lifetime for spontaneous fission decreases near the closed shell nucleus. Experimentally, as general for 8 events out of the 34 synthesized nuclei, spontaneous fission was registered [24]. Particularly, for the isotopes of the element 116 decay chain illustrated in Figure 1.8

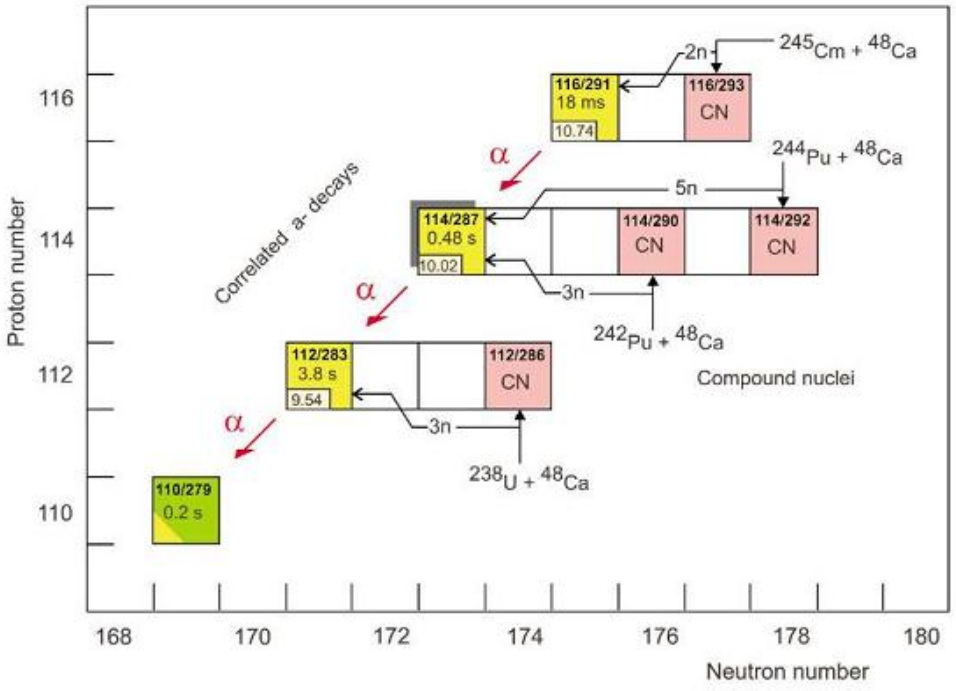

Figure 1.8 Decay chain of SHE 116 [24]

1.11 Uses of super heavy elements [25]:

Despite having numerous features regarding stability or instability of nuclei with in super heavy region, these SHE can be utilized as short lived radioactive species.

As a consequence one may speculate that:

a) They might prove useful as chemical tracers.

b) Some are fantasizing that these SHE may provide the power route necessary for space travel by other life forms with in the universe.

c) An improved understanding of the fission process by studying SHEs will enable scientists to enhance the safety and reliability of the nation's nuclear stockpile and nuclear reactors.

1.12 Current and future experiments

The GSI was to be running an experiment (June 24 – July 25, 2010) to study the formation of ^{293,292}Uuh in the ^{248}Cm(^{48}Ca,xn) reaction as a first step in their future program with a ^{248}Cm target, aiming towards a synthesis of unbinilium (Z=120). The team at Dubna has indicated plans to synthesize ununhexium using the reaction between plutonium-244 and titanium-50. This experiment will allow them to assess the feasibility of using projectiles with Z > 20 required in the synthesis of super heavy elements with Z>118. It is also planned by experimental groups to complete the excitation function of the 4n channel product, ^{292}Uuh, which will allow them to assess the stabilizing effect of the N=184 shell on the yield of evaporation residues. [20]

1.13 References

1. Free Ecylopedia. Chemical elements-element 114 and element 112; transuranium elements.
2. On beyond uranium: journey to the end of the periodic table by Sigurd Hofmann. (Book)
3. Chemistry of super heavy elements by Matthias Schadel. (Book)
4. Island of stability from Wikipedia.
5. R. Freedman, H. Young (2004), University Physics with Modern Physics, 11th

international edition, Sears and Zemansky, 1633-4.

6. Cohen, A.B, concepts of Nuclear Physics, Mc.Graw Hill, 1991.
7. Nuclear shell model from Wikipedia.
8. Peter Armbruster and Gottfried Munzenberg. Creating super heavy elements .scientific American, 34:36–42, 1989.
9. http://www.europhysicsnews.com.
10. Brain R Martin. Nuclear and Particle Physics, An introduction. John Wiley and Sons, Southern Gate, Chichester, West Sussex, England, 2006.
11. Richard F. Casten .Nuclear structure from a simple perspective. Oxford University Press, Biddles Hd, Guildford and Kings Lynn, 2000.
12. S.S. Malik and R.K. Gupta, Phys. Rev. C 39, 1992 (1989).
13. S. K. Arun and R. K. Gupta, DAE Nucl. Phys. (Sambalpur) 52, 365 (2007).
14. Manoj Kumar Sharma, Shefali Kanwar, Gudveen Sawhney, R.K. Gupta and Walter Greiner. J. Phy. G: Nucl.part.phys.38,055104(2011)
15. Gudveen Sawhney, M K Sharma and R.K. Gupta Phy. Rev. C 83,064610 (2011)
16. Wikipedia. Nuclear fusion.
17. Yu.Ts.Oganessian. Reactions of synthesis of heavy nuclei: brief summery and outlook. Physics of atomic nuclei, 69:932–940, 2006.
18. Elements formed by cold and hot fusion from Wikipedia.
19. Peter Moller and J. Rayford Nix. Stability and production of super heavy nuclei preprint [nucl-th9709016].
20. Wikipedia, Ununhexium.
21. Oganessian, Yu. Ts. (2000). "Observation of the decay of {292}116". *Physical Review C* **63**: 011301.
22. Flerov lab annual reports 2000–2006.
23. Yu. Oganessian. Synthesis and decay properties of super heavy elements. Pure and applied chemistry, 78:889–904, 2006.
24. Yuri. Oganessian. Heaviest nuclei from Ca48-induced reactions. Nuclear and Particle Physics, 34:165–242, 2007.
25. Transactinide elements from Wikipedia.

CHAPTER-2 METHODOLGY

Introduction

A comprehensive study of various types of emission from the ground state as well as excited states of compound nucleus (CN) formed in low energy reaction is important, as it gives information about the nuclear structure aside the underlying nuclear forces. At low energies and average nuclear force field acts between decaying fragments which in turns ensure possibility of more than one decay path. This average nuclear force field is largely influenced by entrance channel, angular moment and the temperature consideration along with contribution of deformed and orientation effects.

2.1 Features of DCM

(1) The main aim of the work is to study heavy ion reaction dynamics especially the decay of excited compound nucleus using the dynamical cluster decay model (DCM). [1]- [9]

(2) Deformation and orientation effects of the reaction partner and decay products are explicitly included along with temperature and angular momentum contribution in this model.

(3) The ground state cluster decay of radioactive nuclei has also been undertaken with in the preformed cluster decay model [10]-[18]. Again having deformation and orientation effects of the cluster as well as daughter nuclei included in it.

(4) DCM (dynamical cluster decay model) and PCM (preformed cluster decay model) works alike ,the only difference is DCM for hot and rotating nuclei (i.e. angular momentum and temperature both not equal to zero) preformed cluster model of Gupta and collaborators for ground state decay (ℓ =0,t=0)in cluster radioactive (CR)and related phenomena.[10]

(5) PCM, DCM is also based upon the dynamical (or quantum mechanical) fragmentation theory of cold phenomena in heavy ion reaction and fission dynamics.

(6) The DCM, worked out in terms of the collective coordinates of mass asymmetry

$\eta = (A_1 - A_2)/A_1 + A_2$ and relative separation R respectively gives :-

(a) The nucleon-division (or exchange) between the outgoing fragments.

(b) Transfer of kinetic energy of incident channel (E_{cm}) to internal excitation (total excitation or total kinetic energy, TXE or TKE) of the outgoing channel. It may be noted that the fixed decay point R = R_a (defined later),at which the process is calculated depends upon temperature T as well as on η (i.e.(T, η)) .This energy transfer process can be calculated as follows with the help of

$$E^*_{CN} = E_{c.m} + Q_{in} = IQ_{out}I + TKE(T) + TXE(T) \quad (2.1)$$

The CN excitation E_{CN} is related to temperature T (in MeV) and is given by

$$E^*_{CN} = \frac{1}{9}AT^2 - T(Mev)$$

This model is a two-step model

(a) First step is quantum mechanical preformation probability P_0 of the decay products or cluster formed in the mother nuclei

(b)Second step is the penetration of the fragments/ clusters through the interaction barrier. These two quantities are backbone for calculating cross-section

$$k= \sqrt{\frac{(2\mu Ec.m)}{h^2}}; \sigma = \sum_{l=0}^{lc} \sigma l = \frac{\pi}{k^2}\sum_{l=0}^{lc}(2l+1)PoP \quad (2.2)$$

where $\mu = \frac{A1A2}{A1+A2}m$ reduced mass. m is the nucleon mass.

Preformation probability refers to the motion in mass asymmetry coordinate η = (A_1 - A_2)/A_1+$A_2$the heavy being heavy and light fragments) and the penetrability P to relative separation R motion. Both preformation probability and the penetrability depend on l and T of the system, and on deformations mass $\beta_{\lambda i}$ and orientations θ_i of the two nuclei or fragments. (λ=2, 3, 4, for quadrupole, octupole, hexadecapole deformations)

2.2 How to calculate P_o

The structure information of the CN enters the model via preformation probability Po (also known as spectroscopic factor) of the fragments given by the solution of stationary Schrödinger equation in η.

$$\left\{-\frac{\hbar^2}{2\sqrt{B_{\eta\eta}}}\frac{\partial}{\partial\eta}\frac{1}{\sqrt{B_{\eta\eta}}}\frac{\partial}{\partial\eta}+V_R(\eta,T)\right\}\psi^{\nu}(\eta)=E^{\nu}\psi^{\nu}(\eta) \tag{2.3}$$

With ν =0, 1, 2, 3….referring to the ground state and excited state solution.

For the decay of the hot compound nucleus, we use the postulate of first turning point

$$R_a=R_t+\Delta R\ (T) \tag{2.4}$$

Where

$$R_t = R_1+R_2 \tag{2.5}$$

ΔR(T) is the neck length parameter that assimilates the neck formation effects .This method is introducing a neck length parameter similar to that used in scission point [19] and saddle point[20],[21] statistical fission model. The R_i are radius vectors which are also made temperature dependent can be calculated as

$$R_i(\alpha_i)=R_{0i}\left[1+\sum_{\lambda}\beta_{\lambda i}Y_{\lambda}^{(0)}(\alpha_i)\right] \tag{2.6}$$

With

$$R_{0i}(T) = 1.28A_i^{1/3} - 0.76 + 0.8A_i^{-1/3}\times(1 + 0.0007T^2), \tag{2.7}$$

The corresponding potential V (R_a) acts like an effective Q-value, Q_{eff}, for the decay of the hot

CN at temperature T, to two exit-channel fragments observed in g.s. (T=0), defined by

$$Q_{eff}(T) = B(T) - [B_L(T=0) + B_H(T=0)] = TKE(T) = V(R_a(T)) \quad (2.8)$$

In terms of $Q_{eff}(T)$, the second turning R_b satisfies (see Fig. 2.1)

$$V(R_a, l) = V(R_b, l) = Q_{eff}(T, l) = TKE(T) \quad (2.9)$$

with the l -dependence of R_a defined by

$$V(Ra, l) = Q_{eff}(T, l = 0), \quad (2.10)$$

This means that the R_a, given by Eq. (2.4), is the same for all l -values, and that $V(R_a, l)$ act

Like an effective Q-value, Qeff (T, l), given by the total kinetic energy TKE (T). Then, using (2.9)

R_b (l) is given by the l -dependent scattering potentials, at fixed T as

$$V(R, T, l) = V_c(Z_i, \beta\,\lambda_i, \theta_i, T) + V_p(A_i, \beta\,\lambda_i, \theta_i, T) + V_l(R, A_i, \beta\lambda_i, \theta_i, T) \quad (2.11)$$

Which is normalized to the exit channel binding energy $B_L(T) + B_H(T)$. Such a potential is illustrated in Fig. 2.1, ${}_{20}Ca^{48} + {}_{96}Cm^{248} \longrightarrow {}_{116}{}^{296}$ at $\ell = lmax$ value. The second turning point R_b is marked for the $l = lmax$ ħ case of $R_a = R_t + \Delta R(T)$. The decay path for the l -values begins at $R = R_a$.

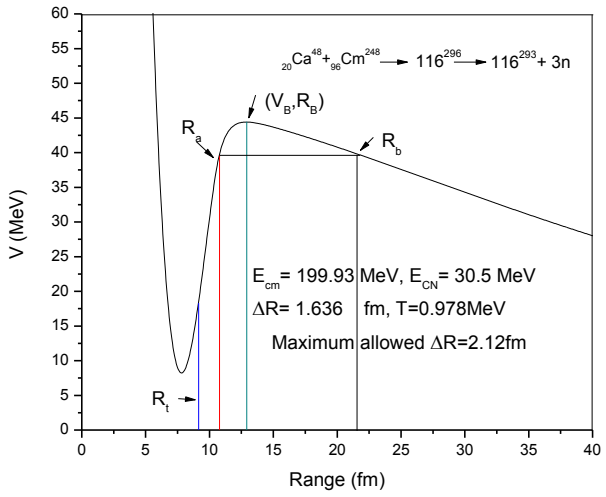

Figure 2.1 Scattering Plot for the reaction ${}_{20}Ca^{48} + {}_{96}Cm^{248} \rightarrow 116^{296}$

The collective fragmentation potential V(R,η,T) in Eq. (2.11) is calculated according to the Strutinsky method by using the T-dependent liquid drop model energy V_{LDM} of [22], with its constants at T=0 re-fitted [3, 4] to give the recent experimental binding energies given by [23], and again refitted [9] to give the recent experimental binding energies[24] and calculate binding energies[25]. Then, including the T-dependence also in Coulomb, nuclear proximity, and *l* dependent potential in complete sticking limit of moment of inertia, we get

$$V(R,\eta,T) = \sum_{i=1}^{2}[V_{LDM}(A_i, Z_i, T) + \sum_{i=1}^{2}[\delta Ui] exp\left(\frac{-T^2}{T_0^2}\right) + V_c(Z_i, \beta_{\lambda i}, \theta_i, T) + V_P(A_i, \beta_{\lambda i}, \theta_i, T) + V_l(R, \beta_{\lambda i}, \theta_i, T) \quad (2.12)$$

Where the T-dependent terms V_c, V_P and V_l are defined as follows: The proximity potential for hot deformed nuclei is [26], [27] (see section 2.3.3)

$$V_p(A_i, \beta_{\lambda i}, \theta i, T) = 4\pi R\,(T)\gamma b(T)\Phi(s_0(T)) \quad (2.13)$$

And, the Coulomb Potential (see section 2.3.4)

$$V_c\left(Z_i, \beta_{\lambda i}, \theta_i, T\right) = \frac{Z_1 Z_2 e^2}{R(T)} + 3Z_1 Z_2 e^2 \sum_{i,i=1,2} \frac{R_i^{\lambda}(\alpha_i,T)}{(2\lambda+1)R(T)^{\lambda+1}}$$

$$Y_{\lambda}^{(0)}(\theta_i)\left[\beta_{\lambda i} + \beta_{\lambda i}^2 Y_{\lambda}^{(0)}(\theta_i)\right] \quad (2.14)$$

With the radius vector given by Eq. (2.6) and surface thickness parameter

$$b\,(T) = 0.99(1 + 0.009T2\,) \quad (2.15)$$

The angular momentum potential, (see section 2.3.5)

$$V_l\,(R, A_i, \beta_{\lambda i}, \theta_i, T) = \frac{\hbar^2\, l\,(l+1)}{2Is(T)} \quad (2.16)$$

With the moment-of-inertia,

$$I_s(T) = \mu R^2 + \frac{2}{5}A_1 m R_1^{\,2}(\alpha_1, T) + \frac{2}{5}A_2 m R_2^{\,2}(\alpha_2, T). \quad (2.17)$$

Further, in Eq. (2.12), within the Strutinsky renormalization procedure, we have defined the binding energy B of a nucleus at temperature T as the sum of liquid drop energy $V_{LDM}(T)$ and shell correction δU (T) i.e.

$$B(T) = V_{LDM}(T) + \delta U \exp(\frac{-T^2}{T_0^2}) \quad (2.18)$$

The T dependent liquid drop part of the binding energy $V_{LDM}(T)$ is from Davidson et al. [22], based on the semi-empirical mass formula of Seeger [28]. For the shell correction δU in Eq. (2.17), since there is no microscopic shell model known that gives the shell corrections for light nuclei, we use the empirical formula of Myers and Swiatecki [29].

After modifying the potential used in above stationary Schrödinger equation, the Schrodinger equation (2.3) can be solved for which the Hamiltonian takes the form:

$$H = \frac{-\hbar^2}{2\sqrt{B_{\eta\eta}}}\frac{\partial}{\partial_\eta}\frac{1}{\sqrt{B_{\eta\eta}}}\frac{\partial}{\partial_\eta} - \frac{\hbar^2}{2\sqrt{B_{RR}}}\frac{\partial}{\partial_R}\frac{1}{\sqrt{B_{RR}}}\frac{\partial}{\partial_R} + V(\eta) + V(R) \quad (2.19)$$

Schrodinger wave equation can be separated for the two co-ordinates η and R as follows,

$$\left[\frac{-\hbar^2}{2\sqrt{B_{\eta\eta}}}\frac{\partial}{\partial_\eta}\frac{1}{\sqrt{B_{\eta\eta}}}\frac{\partial}{\partial_\eta} + V(\eta)\right]\Psi^{\upsilon}(\eta) = E_\eta^{\upsilon}\Psi^{\upsilon}(\eta) \quad (2.20)$$

$$\left[\frac{-\hbar^2}{2\sqrt{B_{RR}}}\frac{\partial}{\partial_R}\frac{1}{\sqrt{B_{RR}}}\frac{\partial}{\partial_R} + V(R)\right]\Psi^{\upsilon}(R) = E_R^{\upsilon}\Psi^{\upsilon}(R) \quad (2.21)$$

With $\psi(\eta, R) = \psi(\eta)\,\psi(R)$

$$E = E_\eta + E_R$$

The states $\Psi^{v}(\eta)$ are the vibrational states in the potential V (η) and are labeled by the quantum numbers ν =0, 1, 2……

In the following subsections, we first discuss the various the various terms of Schrödinger wave equations (2.20) and (2.21) and then give the solution of eq (2.20) for the determination of preformation probability

$$P_0 \propto |\psi^0(\eta)|^2$$

Once the Hamiltonian is established, the Schrödinger equation in mass fragmentation co-ordinate η can be solved. On solving Eq. (2.19) numerically, $|\psi^{v}(\eta)|^2$gives the probability P_0 of finding the mass fragmentation η at a fixed R on the decay path.

$$P0(A2) = |\psi^{v}(A2)|^2 \quad (2.22)$$

For fission studies, like the spontaneous fission and fission through the barrier, the motion in R at the saddle point is adiabatically slow as compared to the η motion. Therefore, the potential is minimized in the neck and deformation coordinates ß1 and ß2 at each R and η values. Starting from the nuclear ground state in spontaneous fission or cluster decay, and to have complete adiabaticity, only the lowest vibrational state ν = 0 is occupied. Then, the mass (or charge) distribution yield, proportional to the probability $|\psi^{(0)}(\eta)|^2$ or $|\psi^{(0)}(\eta_z)|^2$ of finding a certain mass (or charge) fragmentation η (or η Z) at a position R on the decay path, when scaled to, say, mass A2 of one of the fragments (d η =2/A) is given by:

$$Y(A_2) = |\psi_R^{(0)}(A_2)|^2 \frac{2}{A}\sqrt{B_{\eta\eta}(A_2)}).$$

(2.23)

However, if the system is excited or we allow interaction between various degrees of freedom, higher values of ν would also contribute. These enter via the excitation of higher vibrational states, and through the temperature dependent potential V and masses B_{ij}. The effect of adding temperature on potential V and masses B_{ij} is to reduce the shell effects in them, resulting finally in the liquid drop potential V_{LDM} and smoothed (averaged) masses Bij for the systems to be very hot. Apparently, cold fission means taking both the potential V and masses B_{ij} with full shell effects included in them and hot fission means using the V_{LDM} and smoothed (averaged) masses B_{ij}. The possible consequence of such excitations are included here by assuming a Boltzmann like occupation of excited states

$$|\psi(\eta)|^2 = \sum_{\nu=0}^{\infty} |\psi^{\nu}(\eta)|^2 \exp\left(-\frac{E_\eta^\nu}{T}\right)$$

(2.24)

Note that we are dealing here with a directly measurable quantity, the mass (or charge) asymmetry, which works dynamically as mass (or charge) transfer coordinate. Thus, the calculated yields Y (Ai) (or Y (Zi)) are directly comparable with experiments. It may be stressed that there is no free parameter in these calculations. The nuclear shape, once minimized in the neck and deformation coordinates ß1 and ß2 at a given R (=R_{saddle}), remains fixed for both the mass and charge distributions of fission or decay fragments.

2.3 Overview of potentials used in stationary Schrödinger equation

2.3.1The Scattering Potential V(R)

For a fixed η i.e. for a given outgoing fragment (A_1, A_2) combination, the scattering potential V(R) in Eq. (2.11) is defined as the sum of the deformations, orientations dependent coulomb potential, proximity potential and angular momentum dependent potential, i.e.

$$V(R) = V_c(R, Z_i, \beta_{\lambda i}, \theta_i, \Phi) + V_p(R, A_i, \beta_{\lambda i}, \theta_i, \Phi) + V_\ell(R, A_i, \beta_{\lambda i}, \theta_i, \Phi) \quad (2.25)$$

2.3.2 The Fragmentation potential V (η)

The collective potential energy or the fragmentation potential V(η,R), appearing in equation (2.8) is calculated as, $V(\eta,R) = \sum_{i=1}^{2} Bi(Ai, Zi\ \beta\lambda i) + Vc(R, Zi, \beta\lambda i, \theta i, \varphi) + Vp(R, Ai, \beta\lambda i, \theta i, \varphi) + V_l(R, Ai, \beta\lambda i, \theta i, \varphi)$

The fragmentation potential V (η) is calculated at a fixed distance $R=R_1+R_2+\delta R$ or $R=C_1+C_2+\delta C$ fm, with C_i (i=1, 2) as the sussmann central radii related to the radius vector R_i as $C_i = R_i(1-b^2/R_i^2)$ with

$$R_i = R_{0i}[1+\sum_\lambda \beta\lambda i\, Y_\lambda^{(0)}(\alpha i)] \quad (2.26)$$

Here λ=2, 3, 4…. and α_i is an angle that the radius vector R_i of the colliding nuclei makes with the symmetry axis (fig.2.2) the diffuseness of the nuclear surface (I.e. the surface thickness) b =0.99 fm. The charges Z_i are fixed by minimizing the potential V (η) in the η_Z coordinate at each η value.

For the study of excited systems, where the nuclear temperature effects also come into picture, the fragmentation potential at fixed R is

$$V(\eta, T) = \sum_{i=1}^{2} V_{LDM}(A_i, Z_i, T) + \sum_{i=1}^{2} \delta U \exp(-T^2/T^2_0) + V_c(Z_i, \beta_{\lambda i}, \theta_i, \varphi, T)$$

$$+ V_p(A_i, \beta_{\lambda i}, \theta_i, \varphi, T) + V_l(A_i, \beta_{\lambda i}, \theta_i, \varphi, T)$$

Here, $V_{LDM}(A_i, Z_i, T)$ is the liquid drop part of the binding energy and δU, the shell corrections. Note that the calculation of fragmentation potential involves all the possible decay channels and

the number of all such possible decay channels becomes more and more with the increasing mass of the mother nucleus.

2.3.3 The Proximity Potential for deformed, oriented and coplanar nuclei

When two surfaces approach each other within a small distance of less than ~ 2fm, comparable with the surface thickness of interacting nuclei, or when a nucleus is at the verge of dividing into two fragments, then the two surfaces actually face each other across a small gap or crevice. In both cases, the surface energy term alone could not give rise to the strong attraction that is observed when the two surfaces are brought in close proximity. Such additional attractive forces are called proximity forces and the additional potential due to these forces is called the nuclear proximity potential.

Blocki et al. [30] have reanalyzed and extended a theorem, originally due to Deryagin [31], according to which the force between two gently curved surfaces in close proximity is proportional to the interaction potential per unit area between the two flat surfaces. The original expression of Blocki based on the pocket formula was for spherical nuclei, and is given as

$$V_P(s_0) = 4\pi\bar{R}\gamma b\Phi\,(s_0). \tag{2.28}$$

$\Phi\,(s_0)$ is the universal function, independent of the shapes of nuclei or the geometry of nuclear system, but depends on the minimum separation distance

$$\Phi(s_0) = \begin{cases} -1/2(s_0 - 2.54)^2 - (s_0 - 2.54)^3 \\ -3.437\exp(-s_0/0.75) \end{cases} \tag{2.29}$$

respectively, for $s_0 \leq 1.2511$ and $s_0 \geq 1.2511$. Here, s_0 is defined in units of b, i.e. s_0 is s_0/b. This function is defined for negative (the overlap region), zero (touching configuration) and positive values of s_0. For a fixed R, the minimum distance s_0 for spherical nuclei is defined as

$$s_0 = R - R_1 - R_2$$

Where $R = 1.07A_i^{1/3}$(i=1, 2), b is the disuseness of the nuclear surface given by

$$b=[\pi/2\sqrt{3}\ln 9]\ t_{10\text{-}90}$$

Where $t_{10\text{-}90}$ is the thickness of the surface in which the density profile changes from 90% to 10%. The value of b ~1 fm. The γ is the specific nuclear surface tension given by

$$\gamma = 0.9517[1\text{-}1.7826(N\text{-}Z/A)^2]\ \text{Mev fm}^{-2} \tag{2.30}$$

R' is the mean curvature radius of the reaction partners, characterizing the gap; this for spherical nuclei is given by

$$\overline{R} = R_1R_2 / R_1 + R_2$$

2.3.4 The Coulomb potential

Coulomb potential describes the force of repulsion between two interacting nuclei due to their charges. It acts along the line joining the two nuclei. The Coulomb potential for two interacting spherical nuclei is given as

$$V_c = Z_1Z_2e^2/R$$

For interacting deformed and oriented nuclei, different authors [32]-[36] have derived it differently. In this thesis work, we have started with Coulomb potential of Wong [35], given for two non-overlapping charge distributions, having quadruple deformations only, i.e.

$$V_c = \frac{Z_1 Z_2 e^2}{R} + \left(\frac{9}{20\pi}\right)^{1/2}\left(\frac{Z_1 Z_2 e^2}{R^3}\right)\sum_{i=1}^{2} R_i^2(\alpha_i)\beta_{2i}P_2(cos\theta_i) + \left(\frac{3}{7\pi}\right)\left(\frac{Z_1 Z_2 e^2}{R^3}\right)\sum_{i=1}^{2} R_i^2(\alpha_i)\left[\beta_{2i}P_2(cos\theta_i)\right]^2 \tag{2.31}$$

in this expression, the quadrupole-quadrupole interaction term, proportional to $\beta_{21}\beta_{22}$, is neglected since it has a short-range character. For nuclei lying in the same plane we have generalized it to include the higher order deformations (λ = 3, 4...), obtaining

$$V_c(Z_i, \beta_{\lambda i}, \theta_i, T) = \frac{Z_1 Z_2 e^2}{R(T)} + 3Z_1 Z_2 e^2 \sum_{\lambda,i=1,2} \frac{R_i^{\lambda}(d_i,T)}{(2\lambda+1)R(T)^{\lambda+1}}.$$

2.3.5 Rotational Energy due to angular momentum

The rotational motion gives an additional energy due to the angular momentum define as

$$V_l = \frac{h^2 l(l+1)}{8\pi^2 I} \quad (2.32)$$

With $I = \mu R^2$, is the non-sticking limit of moment of inertia with as the $\mu = ((A_1A_2) / (A_1+A_2))$ m reduced mass m is the nucleon mass. In the complete sticking limit, the moment of inertia I is given as,

$$I = \mu R^2 + 2/5 A_1 m R_1^2 + 2/5 A_2 m R_2^2 \quad (2.33)$$

With R_i from Eq. (2.32). However, for the relative separation of interest here, we use the sticking limit. It is relevant to mention here that value of angular momentum extracted experimentally, is based upon moment of inertia limit.

Another two important terms regarding DCM

2.4 Penetration Probability P

Penetrability P measures the capability of fragments nucleus to penetrate the potential barrier generalized during compound nucleus formation. The penetrability P is the WKB integral between R_a and R_b.

$P=\exp [-2/h \int_{Ra}^{Rb} \{2\mu [V(R)-Q_{eff}]\}^{1/2} dR]$, with R_b as the second turning point , satisfying

$$V(Ra, l) = V(R_b, l) = Q_{eff}(T, \ell = \ell_{min}) = TKE(T),$$

Which means that the potential $V(R_a, \ell)$, correspond to R*a* ,acts like an effective Q-value, $Q_{eff}(T, \ell = \ell_{min})$,in the WKB integral, and gives the total kinetic energy TKE(T), where $\ell_{min}=0$ or refers to the minimum ℓ-value that starts to contribute to WKB integral.

2.5 References

[1] R.K. Gupta, M. Balasubraniam, C. Mazzocchi, M. La Commara, and W.Scheid, Phys. Rev. C 65, 024601 (2002).

[2] M.K. Sharma, R.K. Gupta, and W. Scheid, J. Phys. G 26, L45 (2000).

[3] R.K. Gupta, R. Kumar, N.K. Dhiman, M. Balasubraniam, W. Scheid, and C.Beck, Phys. Rev. C 68, 014610 (2003).

[4] M. Balasubraniam, R. Kumar, R.K. Gupta, C. Beck, and W. Scheid, J. Phys. G 29, 2703 (2003)

[5] R.K. Gupta, M. Balasubraniam, R. Kumar, D. Singh, and C. Beck, Nucl.Phys. A 738, 479c (2004).

[6] R.K. Gupta, M. Balasubramaniam, R. Kumar, D. Singh, C. Beck, and W.Greiner, Phys. Rev. C 71, 014601 (2005).

[7] B.B. Singh, M.K. Sharma, R.K. Gupta, and W.Greiner, Int.J. Mod.Phys.E15,699 (2006)

[8] R.K. Gupta, M. Balasubraniam, R.Kumar, D.Singh, S. K. Arun and W.Greiner, J.Phys .G:Nucl.Part. Phys. 32, 345(2006)

[9] B.B. Singh, M.K. Sharma, R.K. Gupta, Phys.Rev. C 77, 054613 (2008)

[10] R.Gupta, in proceedings of the 5^{th} International Conference on Nuclear Research Mechanics, Varenna, 1988, edited by E. gladioli , (Ricerca Scientifica ed Educazione Permanente ,Milano, 1988),p.416.

[11] S.S. Malik and R.K.Gupta, Phys.Rev.C 39, 1992(1989)

[12] R.K.Gupta, W.Scheid, and W.Greiner, J.Phys.G: Nucl. Part. Phys. 17, 1731(1991).

[13] S. Kumar and R.K.Gupta, Phys.Rev. C 49, 1922(1994).

[14] R.K.Gupta and W. Greiner Int. J. Mod. Phys. E 3, 335 (1994, Suppl.).

[15] S. Kumar and R.K.Gupta, Phys. Rev. C 55, 218 (1997).

[16] R.K. Gupta, in Heavy Elements and Related New Phenomena ,edited by W.Greneir and R.K Gupta (World Scientific Singapore) Vol.II ,p.730

[17] S.K and R.K Gupta, DAE nucl.Phys. (Sambalpur) 52,365(2007)

[18] B.B.Singh, S.K Arun, M.K.Sharma, S.Kanwar and Raj K.Gupta, DAE Nucl.Phys. (Roorkee), Accepted (2008)

[19] T. Matsuse, C. Beck, R. Nouicer, and D. Mahboub, Phys. Rev. C 55, 1380 (1997).

[20] S.J. Sanders, D.G. Kovar, B.B. Back, C. Beck, D.J. Henderson, R.V.F. Janssens, T.F. Wang, and B.D. Wilkins, Phys. Rev. C 40, 2091 (1989t).

[21] S.J. Sanders, Phys. Rev. C 44, 2676 (1991).

[22] N.J. Davidson, S.S. Hsiao, J. Markram, H.G. Miller, and Y. Tzeng, Nucl. Phys. A 570, 61c (1994).

[23] G. Audi and A.H. Wapstra, Nucl. Phys. A 595, 4 (1995).

[24] G. Audi and A.H. Wapstra and C. Thiboult, Nucl. Phys. A 729, 337(2003).

[25] P. M¨oller, J. R. Nix, W. D. Myers, and W. J. Swiatecki, At. Data Nucl. Data Tables 59, 185 (1995).

[26] R.K. Gupta, N.Singh, and M. Manhas, Phys. Rev. C 70, 034608 (2004)

[27] R.K. Gupta ,M.balasubramaniam, R.Kumar, N.Singh, M.Manhas, and W. Greiner, J.Phjs. G: Nucl.Part. Phys. C 31, 631(2005).

[28] P. A.Seeger, Nucl. Phys. 25, 1 (1961)

[29] W. Myers and W.J. Swiatecki, Nucl. Phys. 81, 1 (1966).

[30] J. Blocki, J. Randrup, W. J. Swiatecki, and C. F. Tsang, Ann. Phys. (NY) 105,427 (1977).

[31] Deryagin, Kolloid Z. 69, 155 (1934).

[32] N. Malhotra and R.K. Gupta, Phys. Rev. C 31, 1179 (1985).

[33] M M¨unchow, D Hahn and W Scheid, Nucl. Phys. A 388, 381 (1982).

[34] M J Rhoades-Brown, V E Oberacker, M Seiwert and W Greiner, Z. Phys. A 310, 287 (1983).

[35] C Y Wong, Phys. Rev. Lett. 31, 766 (1973).

[36] R Aroumougame and R K Gupta, J. Phys. G: 6, L155 (1980).

Chapter-3

3.1 Results and discussions

The decay of $^{296}116$ formed in $^{48}Ca + ^{248}Cm$ reaction has been studied experimentally and the fusion evaporation residue cross-section have been measured at excitation energies $E_{CN} \approx 30 - 40$ MeV [1]. We have studied the reaction $^{48}Ca + ^{248}Cm \rightarrow 116^{296}$ by taking Z=126, N=184 magic shell closures in the super heavy region as suggested by [2] in order to understand the decay path of super heavy system 116^{296}. Although Z=114 & Z=120 are also considered as one of the possible magic number in super heavy region but Z=126 seems more suitable with in domain of Dynamical Cluster Decay Model approach to account for decay path of nuclear systems formed in heavy ion reactions.

(1) First of all, we try to fit the cross-section of $^{296}116$ using spherical fragmentation at three different compound nucleus energies E_{CN} = 30.50 MeV, 32.71 MeV, 38.59 MeV for 3n decay. The value of the calculated cross-section was less than the experimental data even at maximum allowed ΔR (2fm). ΔR, the neck length parameter is the only parameter of DCM and ΔR_{max}= 2fm is taken in reference to the nuclear interaction potential involved in DCM calculations. The table 3.1 shows the comparison between the calculated and experimental value. Therefore using spherical fragmentation the available experimental cross-sections could not be fitted.

Energy (MeV)	σ_{3n}(DCM, Spherical) (barn)	σ_{3n}(Experimental value) (barn)
30.50	1.44 E-17	.879 E-12
32.71	1.34 E-15	.514 E-12
38.59	6.40 E-14	1.186 E-12

Table3.1

From here we conclude that spherical fragmentation did not work in the DCM framework for the decay of 116^{296} so the deformations effect seems essential for the study of this nuclear system.

It may be relevant that ^{48}Ca is spherical projectile but it is being hit at a deformed target ^{248}Cm with (β_2=0.235, β_3=0, β_4=0.008) so the fragmentation path of compound system seem to be governed in reference to different deformed fragmentation possibilities and it seems that in corporation of deformation effects of all possible fragment masses is extremely desirable in order to study the decay path of super heavy nucleus Z=116, N=180 (A=296).

(2) Keeping this in mind we tried to fit the cross-section of this reaction using quadrupole (β_2) deformations and compare it with the experimental data. The comparison between the experimental values and corresponding calculated values using deformation effects up to β_2 at their corresponding ΔR are given in table 3.2.

Energy (MeV)	ΔR (fm)	ℓ_{max}	σ_{3n}(DCM,Hot-fusion) (pb) (barn)	σ_{3n} (experimental) (pb) (barn)
30.50	1.636	123	.877	.879
32.71	1.519	130	.512	.514
38.59	1.481	138	1.18	1.186

Table 3.2

The figure 3.1 shows the comparison of deformed choice of fragmentation with spherical one at E_{CN}=32.71MeV. One may clearly see that mass fragmentation is relatively smooth with spherical choice (no strong dips are reported) whereas with β_2, there seems to be more structure in fragmentation path. The comparison is done at same excitation and center of mass energy, with same Δ R=1.519. The maximum angular momentum ℓ_{max} is relatively small as compared to that for deformed fragmentation. For the further analysis we shall concentrate only on the deformed fragmentation as the experimental cross-sections could be fitted only with the inclusion of deformed effects.

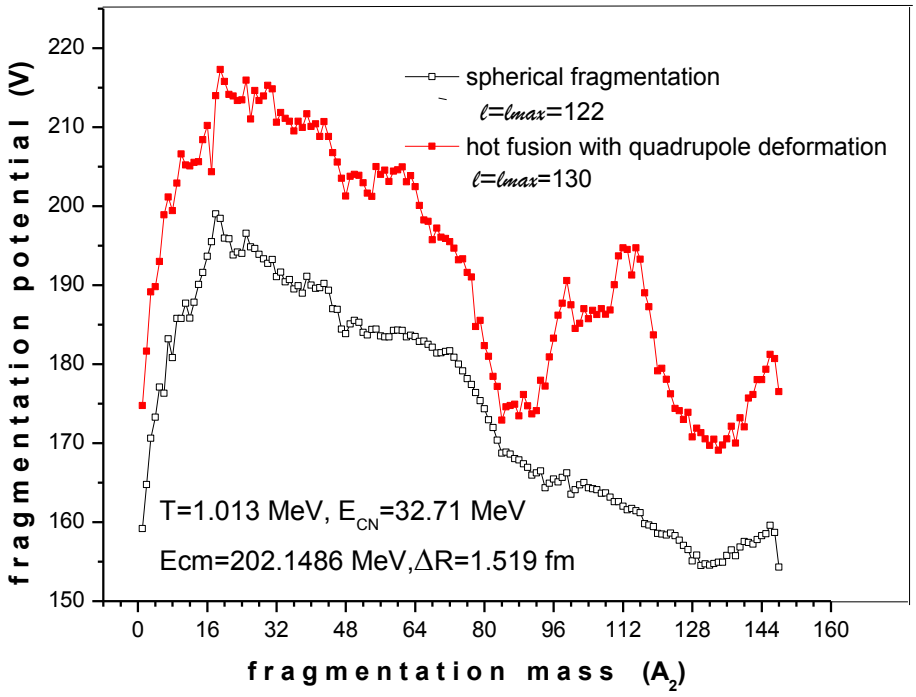

Figure 3.1 fragmentation potential as a function of fragmentation mass for spherical fragment and hot fusion (with quadrupole deformations).

Figure 3.2 shows the variation of preformation probability as a function of fragmentation mass for spherical fragmentation and fragmentation system for deformed system (β_2). The calculations are done at the same compound nucleus energy (E_{CN}=32.71 MeV), same ΔR (1.519 fm) with temperature value 1.013 MeV. The value of ℓ_{max} in case of spherical fragmentation is 122ħ and in case of hot fusion is 130ħ and the figure shows variation at their corresponding ℓ_{max}*'s*. One pointed of interest here is that the fragmentation path seems to become more symmetric for spherical fragmentation as compared to that for deformed case. However, it is a very preliminary to draw definite conclusion as the experimental data is fitted only for deformed path.

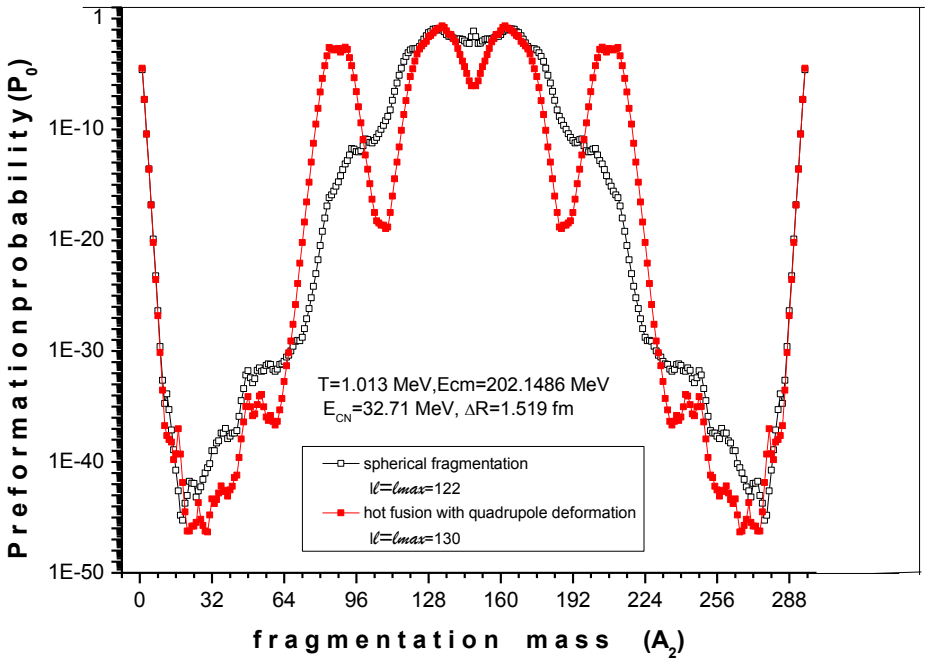

Figure 3.2 Variation of preformation probability for spherical fragmentation and hot fusion (with β_2 effect) at same energy and ΔR.

Figure 3.3 shows the mass fragmentation potential V (A_2) for the compound nucleus $^{296}116$ at ΔR=1.519 fm at T= 1.013 MeV corresponds to one of the compound nucleus energy E_{CN}=32.71MeV using quadrupole deformation β_2 with magic number for super heavy region as Z=126 and N= 184 for two extreme angular momentum values i.e. at $\ell = 0$ and $\ell = \ell_{max}$. The ℓ_{max} is decided at a point where the cross-sections of light particle fragment (3n in this case) become negligibly small.

In the figure, for 80<A<94 and 128<A<140, we see an enhanced minima's for $\ell = 0$ as well as $\ell = \ell_{max}$ case. These minima's clearly show the dominance of these fragments as decay products at least on the basis of fragmentation potential.

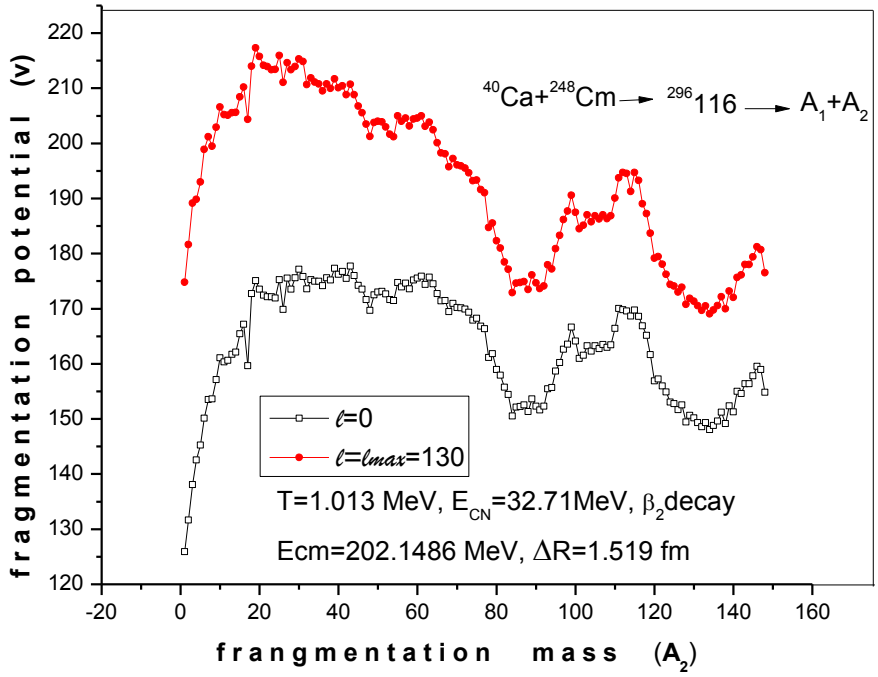

Figure3.3: fragmentation potential as a function fragmentation mass at $\ell = 0$ and $\ell = \ell_{max}$

Figure 3.4 shows the variation of preformation probability P_0 as a function of fragment mass number, calculated at $\ell = 0$ and $\ell = \ell_{max}$ =130ħ and ΔR=1.519 at temperature T=1.013. Maximum preformation probability is equal to 0.4899 ($\ell = \ell_{max}$) is seen for fragments mass 134 and 162. Clearly the mass fragmentation is asymmetric with fairly large contribution of fragments in the vicinity of fragmentation mass 128-168 i.e. (A/2) ±20. The fission fragmentation is near symmetric for two extreme cases of angular momentum. It is relevant to mention here that Preformation probability P_0 is the important ingredients' of DCM and it seems to impart important nuclear structure information.

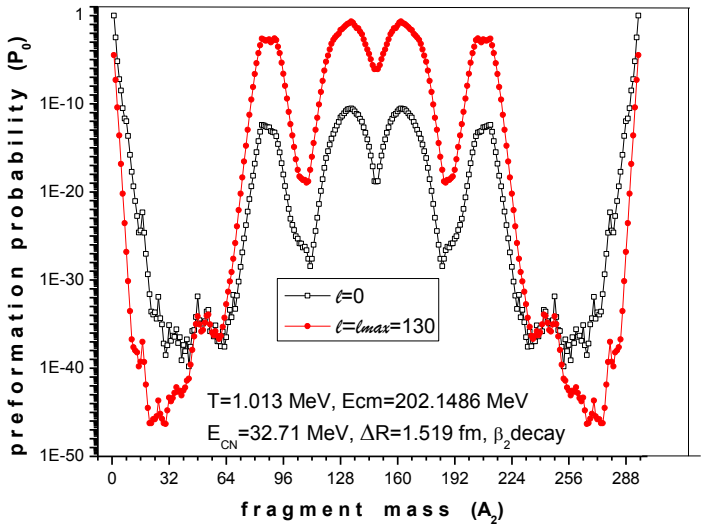

Figure3.4: Variation of Preformation probability (P_0) as function of Fragment Mass (A_2) at $\ell = 0$ and $\ell = \ell_{max} = 130$

The figure 3.5 shows the fragmentation potential variation as a function of fragmentation mass at the three different compound nucleus energies E_{CN}=30.50 MeV, 32.71MeV, 38.59 MeV, for which we fit the cross-sections. The values of their corresponding fittings ΔR and ℓ_{max}'s are given in figure. The details of which can also be seen in Table 3.2.

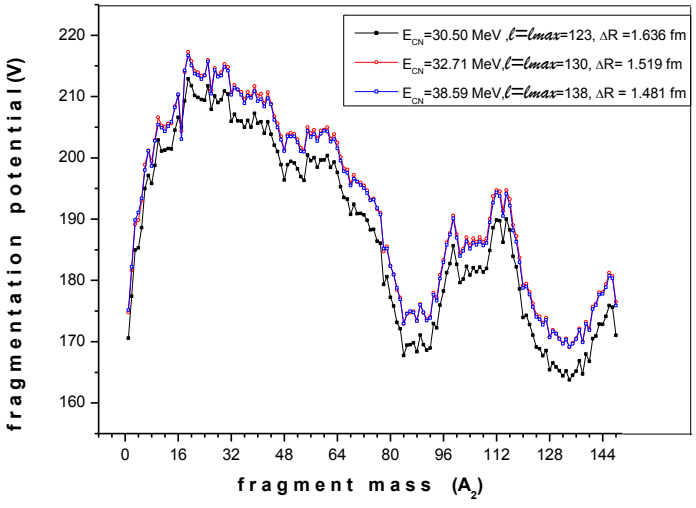

Figure 3.5 fragmentation potential variations as a function of fragmentation mass at different energies.

From figure 3.5 we can say that for the three chosen energies the variation of fragmentation potential as a function of fragmentation mass shows almost similar behavior with small change in the magnitude of fragmentation potential. For example at 32.71 MeV there is higher value of fragmentation potential w.r.t other energies.

Figure 3.6 shows the variation of preformation probability as a function of fragmentation mass at three different energies, for which the 3n cross-sections have been fitted. One can clearly see from figure 3.6 that the potential energy surfaces (PES) remains unaffected with increase in compound nucleus energy.

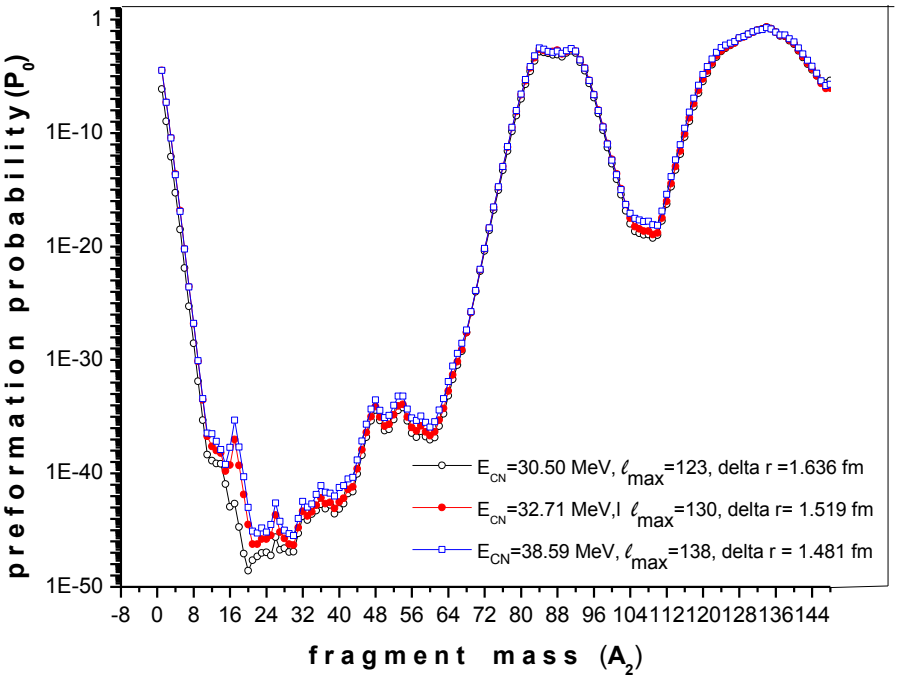

Figure 3.6 Variation of preformation probability as a function of fragmentation mass at different energies.

In other words for three chosen energies the variation path of preformation probability as a function of fragmentation mass is almost same.

The graph 3.7 shows the variation of cross-sections (calculated and experimental) with E_{CN}.

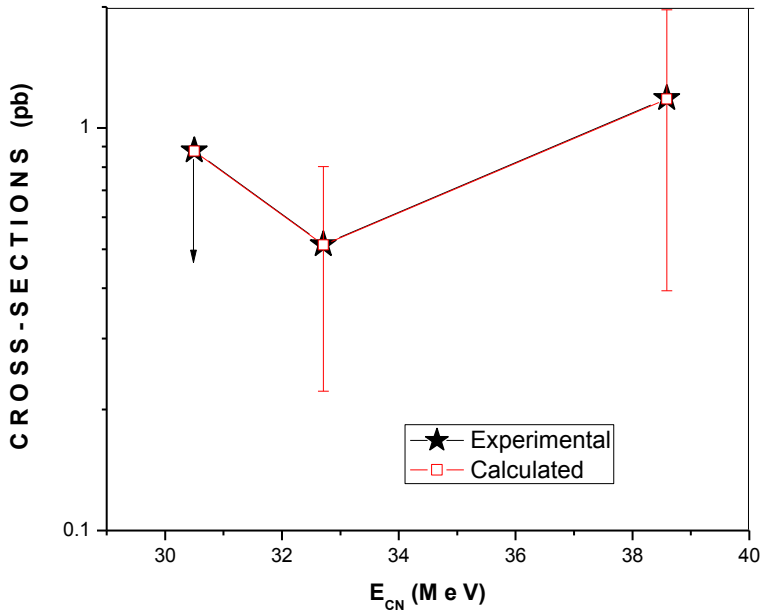

Figure 3.7: Variation of cross-section with E_{CN}

From this graph 3.7 and table 3.2, it is clear that experimental and DCM cross-sections match nicely with inclusion of deformations up to β_2.

Then we tried to fit the fusion evaporation residue cross-section for the same reaction for 4n decay channels. We have calculated the 4n cross-sections at given compound nucleus energy E_{CN}= 39.18MeV, and the corresponding values of E_{cm} =208.6186 MeV, temperature T=1.107MeV. To fit the fusion evaporation residue cross-section first of all we find the value of maximum allowed ΔR (~2fm as discussed before).

By taking maximum value of ΔR, we tried to fit the cross-sections for the 4n decay path. From calculations we find that even at maximum value of allowed ΔR (2fm) the calculated value of fusion evaporation residue cross-sections are underestimated by the factor of 2. To be precise, the calculated value of cross-section at maximum allowed ΔR (2fm) is 0.188pb and experimental is 3.39pb.

In conclusion, 3n decay cross-sections are fitted nicely for $^{296}116$ nucleus with inclusion of deformations effects up to quadrupole deformations (β_2). The spherical fragmentation doesn't seem to work for this super heavy nucleus. However 4n decay cross-sections could not be fitted with in the frame work of DCM which calls for role of higher multipole deformations (up to hexadecapole) or may try the improved version of liquid drop energy for super heavy region as suggested by [3].

3.2 References

1. Yu. Ts. Oganessian et. al. Physics Review C, 70, 064609 (2004).
2. Raj K Gupta, Niyti and Walter Greiner, j. phys. G: nucl. Part Phys .37 (2009)
3. Tiekuang Dong and Zhongzhou Ren, Physics Review C77, 064310 (2008).